Deep Learning Architecture For Brain Vessel Segmentation

Khadija Iddrisu[1] and **Alessandro Crimi**[2]

African Masters of Machine Intelligence[1], Sano Center For Computational Medicine [2]

Introduction

We explore and propose an automated method for brain vessel segmentation to alleviate the following identified problems:

- Difficulty and delay in manual vessel segmentation due low contrast images from medical imaging processes.
- Health Hazards of contrast enhancing dyes
- Cost involved in manual brain vessel segmentation

A transfer learning approach is adapted to perform vessel segmentation of the human brain [1].

Convolutional Neural Networks (CNN)

CNNs are the main deep learning structures used in image processing and the main architectures used in this task. They consist of several layers for different purposes illustrated below.

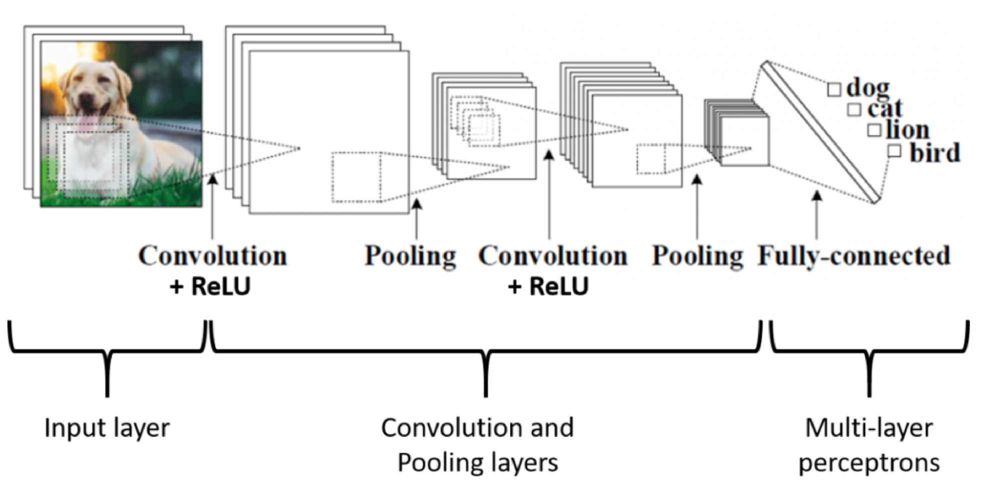

Fig. 1: CNN Architecture [2]

Mathematically, the continuous convolution of two functions in 1 dimension is expressed by;

$$f(t) * g(t) = \int_0^t f(\tau)g(t-\tau)d\tau. \qquad (1)$$

Convolutions have several properties including:

- Commutativity
$$f * g = g * f; \qquad (2)$$
- Associativity
$$f * (g * h) = (f * g) * h; \qquad (3)$$
- Distributivity
$$f * (g + h) = (f * g) + (f * h). \qquad (4)$$

A special type of CNN, the Fully Convolutional Network(FCN) is mostly used in segmentation tasks. A common filter applied for this task is the edge detection filter illustrated below.

Fig. 2: Convolution on Circle of Wilis

BackBone Model Architecture

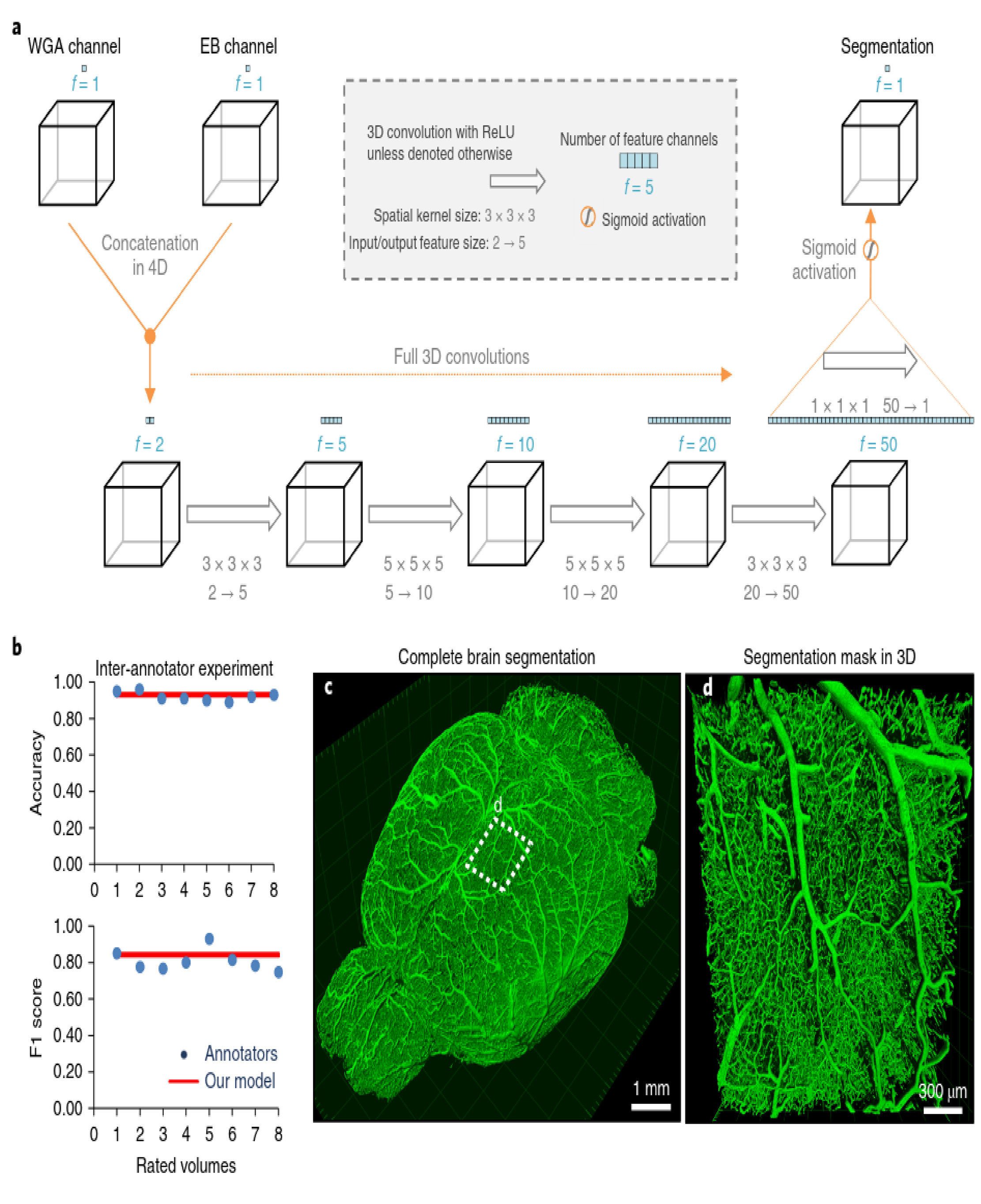

Fig. 3: Vessap Architecture [3].

Transfer Learning

We perform transfer learning as a method to solve the unavailability of manually annotated images. This approach allows us to start with learned features before adjusting these features to suit the specific segmentation task we want to carry out instead of starting the process all over from scratch.

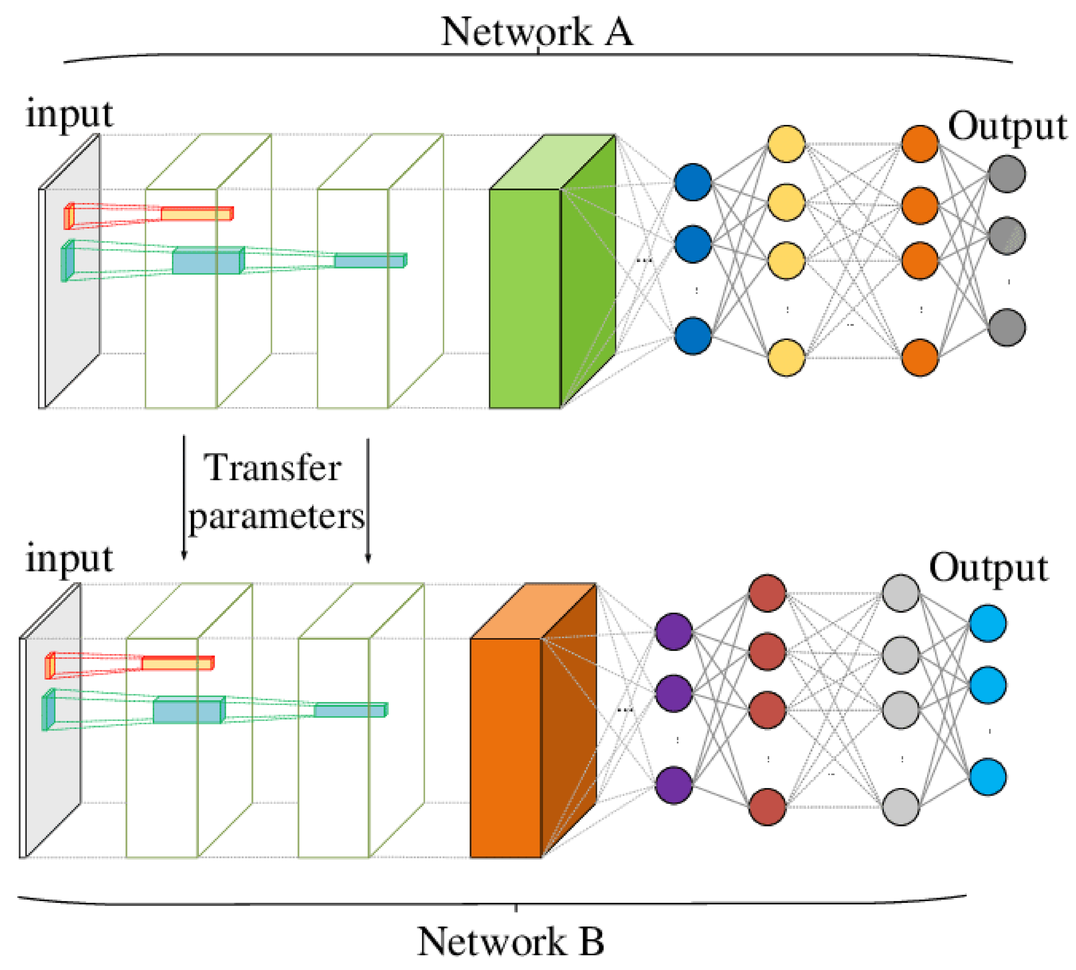

Fig. 4: Illustration of transfer learning [4].

Our approach mainly involved hyper-parameter tuning to enable the deep learning architecture to work on our task of human brain segmentation

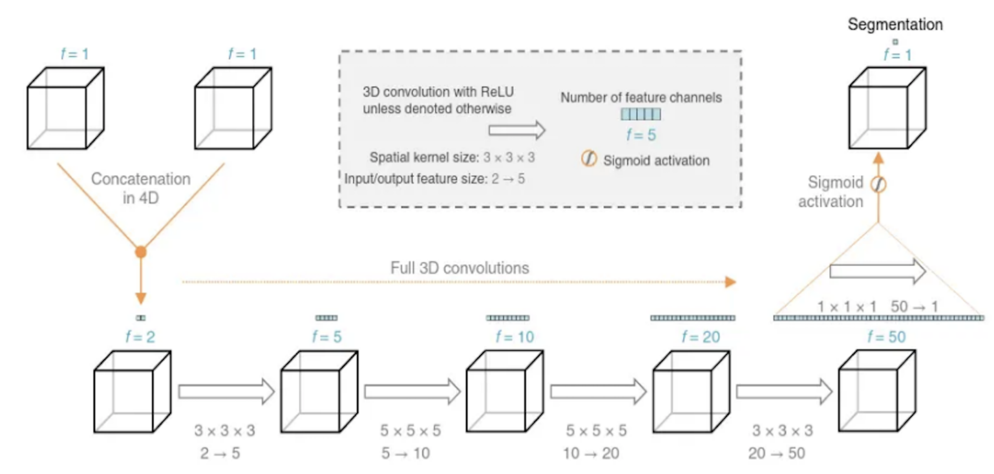

Fig. 5: Illustration of pre-trained model

Vessap Model Vs Fine-tuned Model		
Data	Volumes of Mouse Brain	Volumes of Human Brain
Input	Images stained with dye	Low contrast MRA images concatenated
Execution time	5 minutes execution time	4 minutes execution time
Crosshair filters	False	True
Normalize Data	Max	Max
Input Channel	2	1
Batch size	10	12
learning rate	0.01	1
Cube size	64	32
Threshold	0.5	0.6
Optimizer	Adam	SGD

The class balancing loss function with stable weights is implemented to account for general class imbalances.

$$L(W) = L(W_1) + L(W_2)$$
$$L_1(W) = -\frac{-1}{|Y_+|}\sum_{j\in Y_+} logP(y_j = 1|X;W) - \frac{1}{|Y\_|}\sum_{j\in Y\_} logP(y_j = 0|X;W)$$
$$L_2(W) = -\frac{\gamma_1}{|Y_+|}\sum_{j\in Y_{f+}} logP(y_j = 0|X;W) - \frac{\gamma_2}{|Y\_|}\sum_{j\in Y_{f\_}} logP(y_j = 1|X;W)$$

$$\gamma_1 = 0.5 + \frac{1}{Y_{f+}}|\sum_{j\in Y_{f+}} P(y_j = 0|X;W) - 0.5|$$

$$\gamma_2 = 0.5 + \frac{1}{Y_{f\_}}|\sum_{j\in Y_{f\_}} P(y_j = 1|X;W) - 0.5|$$

Evaluation

Evaluation metrics of the different segmentation approaches for 75 volumes of 100 × 100 × 50 pixels (s:seconds).

Segmentation model	CI-F1	Accuracy	F1-Score	Jaccard	Parameters	Speed
VesSAP CNN	**0.93 ± 0.02**	**0.94 ± 0.01**	**0.84 ± 0.05**	**0.84 ± 0.04**	**0.0587 m**	**1.19 s**
VesSAP CNN, trained from scratch	**0.93 ± 0.02**	**0.94 ± 0.01**	**0.85 ± 0.04**	**0.85 ± 0.04**	**0.0587 m**	**1.19 s**
VesSAP CNN, synthetic training data	0.87 ± 0.02	0.90 ± 0.05	0.72 ± 0.07	0.70 ± 0.05	**0.0587 m**	**1.19 s**
3D U-Net	**0.93 ± 0.02**	**0.95 ± 0.01**	**0.85 ± 0.03**	**0.85 ± 0.03**	178.4537 m	61.22 s
V-Net	**0.94 ± 0.02**	**0.95 ± 0.02**	**0.86 ± 0.07**	**0.86 ± 0.07**	88.8556 m	26.87 s
Frangi Vesselness	0.84 ± 0.03	0.85 ± 0.03	0.47 ± 0.19	-	-	117.00 s
Markov Random Field	0.86 ± 0.02	0.85 ± 0.03	0.48 ± 0.04	-	-	24.31 s

Fig. 6: Vessap Results [5].

Qualitative Results

VesSAP enables reliable segmentation and feature extraction (bifurcation points, radius and centerlines) down to the capillary-level from the imaging data. We provide results of the segmentation of the Vessap Model as well as results of our pre-trained model.

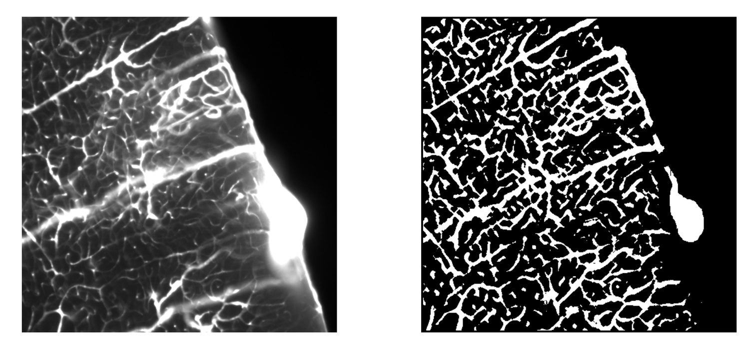

Fig. 7: Original and Segmented Slices of Vessap Segmentation

Fig. 8: Original and Segmented Slices of ABDIV Data

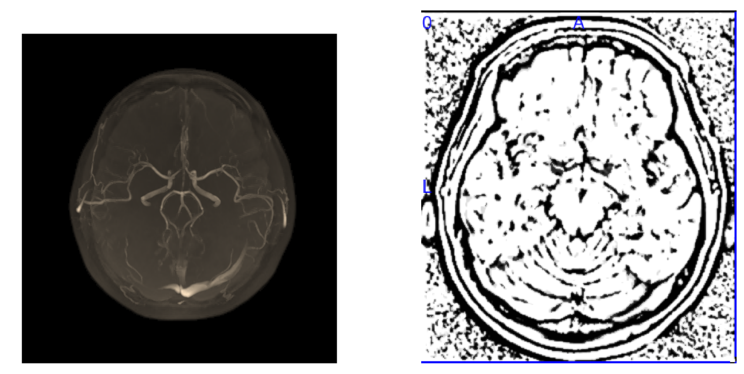

Fig. 9: Original and Segmented Slices of MRA Data

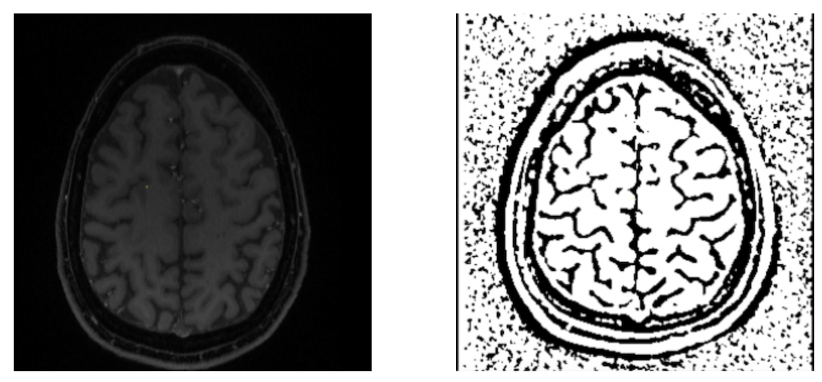

Fig. 10: Original and Segmented Slices of IXE Data

Metrics and Features Extracted		
Features/Metric	MRA Data	IXE Data
Loss	7.9870e-07	6.9870e-07
Metric	0.9	0.8
Centerlines	True	True
Max Radius	18.98	17.42
Min Radius	3.82	2.96
Skeleton Length	63934	43934
Bifurcations	9725	8742

Code and Implemenatation

The entire experiment was run using the Code-Ocean public Capsule. To perform segmentation and generate results, we make a copy of the Vessap public capsule and train our model.

Acknowledgements

My sincere gratitude goes to AIMS Ghana for giving me this opportunity to work on this project. I will also like to express my appreciation to my supervisor Dr. Alessandro Crimi for his support. Lastly, I will like to thank the organizers of this workshop as well as the Deep Learning Indaba committee for giving me this opportunity to showcase my research.

References

[1] Lisa Torrey and Jude Shavlik. "Transfer learning". In: *Handbook of research on machine learning applications and trends: algorithms, methods, and techniques*. IGI global, 2010, pp. 242–264.

[2] *KDNuggets Using Topological Data Analysis to Understand the Behavior of Convolutional Neural Networks*. https://www.kdnuggets.com/2018/06/topological-data-analysis-convolutional-neural-networks.html. Accessed: 2010-09-30.

[3] Mihail Ivilinov Todorov et al. "Machine learning analysis of whole mouse brain vasculature". In: *Nature methods* 17.4 (2020), pp. 442–449.

[4] Joseph Lemley, Shabab Bazrafkan, and Peter Corcoran. "Transfer Learning of Temporal Information for Driver Action Classification." In: *MAICS*. 2017, pp. 123–128.

[5] Giles Tetteh et al. "Deepvesselnet: Vessel segmentation, centerline prediction, and bifurcation detection in 3-d angiographic volumes". In: *Frontiers in Neuroscience* (2020), p. 1285.